Annals of Emerging Technologies in Computing (AETiC)
Vol. 9, No. 1, 2025

Research Article

Research on Unmanned Path Planning of Intelligent Vehicle Based on Swarm Intelligence Algorithm

Tao Yang[1] and Dandan Song[1,2,*]

[1]Henan Vocational and Technical College of Communications, China
yt13674948098@163.com
[2]Changsha University of Science Technology, China
dandansong66@163.com
*Correspondence: dandansong66@163.com

Received: 14th February 2024; Accepted: 27th December 2024; Published: 1st January 2025

Abstract: Unmanned vehicles represent a significant advancement in automotive technology, with their development hinging on sophisticated perception, decision-making, and control capabilities. However, existing path planning methods for driverless cars face challenges in complex road environments due to their susceptibility to environmental factors. This paper aims to address this issue by first providing an overview of trajectory planning algorithms for driverless cars. Subsequently, a novel global path planning approach is proposed, leveraging an improved A* algorithm and a predictive model of travel time. The proposed method enhances path planning accuracy by integrating the A* algorithm with predictive capabilities regarding travel time. By considering not only the shortest path but also the anticipated time required to traverse it, the model can account for dynamic factors such as traffic congestion and road conditions. This predictive aspect adds a layer of adaptability to the path planning process, enabling intelligent vehicles to make informed decisions in real-time. Simulation results demonstrate the efficacy of the proposed model in accurately planning trajectories for intelligent vehicles. The research results indicate that the prediction results of the bidirectional LSTM network are highly consistent with the actual values, demonstrating good predictive ability. From the perspective of prediction error, the MAE (Mean Absolute Error) of the bidirectional LSTM model is 7.3165, which is superior to the other three models. Especially compared with unoptimized BPNN, bidirectional LSTM reduced MAE, MAPE, and RMSE by 32%, 38%, and 3%, respectively, which fully demonstrates the advantages of bidirectional LSTM in processing time series data. It can accurately predict the inflow of road segments in real time and calculate the travel time of a future road segment.

Keywords: ***Autonomous driving; Bidirectional LSTM network; Path planning; Predicting inflow volume; Swarm intelligence algorithm; Vehicle trajectory***

1. Introduction

Data mining is a comprehensive field that integrates multiple disciplines such as business intelligence (BI), data analysis (DA), big data (BD), and decision support (DS). These fields are all products of the cross integration of data mining technology with other industries [1]. Data mining has the ability to predict future trends or overall development directions, which helps us make proactive predictions, reveal hidden patterns and correlations behind data, and make decisions faster and more accurately. Especially in the field of transportation, especially in densely populated and complex central cities with intricate road networks, scientific planning, road construction evaluation, design of sidewalks, overpasses, underground passages, and layout of subway stations all urgently require data support [2]. Scientific and rational planning and layout are crucial for achieving the intelligence and convenience of cities. With the continuous growth of the number of cars, urban traffic congestion is becoming increasingly severe, and traffic accidents occur

Tao Yang, Dandan Song, "Research on Unmanned Path Planning of Intelligent Vehicle Based on Swarm Intelligence Algorithm", *Annals of Emerging Technologies in Computing (AETiC)*, Print ISSN: 2516-0281, Online ISSN: 2516-029X, pp. 73-86, Vol. 9, No. 1, 1st January 2025, Published by International Association for Educators and Researchers (IAER), DOI: 10.33166/AETiC.2025.01.005, Available: http://aetic.theiaer.org/archive/v9/v9n1/p5.html.

frequently, resulting in a large number of casualties and huge economic losses every year. The frequent occurrence of traffic accidents, worsening traffic congestion, and severe environmental pollution have jointly promoted the rapid development of autonomous vehicle technology [3].

Driverless cars contain many advanced technologies, including computers, automatic control, and artificial intelligence technologies [4]. Because of its good autonomous driving function, driverless cars can effectively perform driving tasks in complex and dangerous environments and have good application value in many fields. Path planning is one of the core technologies in the research and development of unmanned vehicles. Its task is to obtain a safe and collision-free trajectory to ensure that the vehicle can safely reach the target point from the starting point along the trajectory [5]. In the process of travelling, the unmanned vehicle needs to avoid dynamic and static obstacles while ensuring the shortest path to achieve energy optimization. The increasing progress of driverless, smart car technology is not only conducive to alleviating traffic congestion but also reducing casualties caused by car accidents, realizing the research value in the automotive industry [6]. As the key to unmanned vehicles, the development of path-planning technology will definitely promote the qualitative leap of unmanned vehicle technology, which has very important research significance and application prospects [7].

This article aims to address the challenges faced by autonomous vehicles in path planning in complex road environments, particularly their sensitivity to environmental factors. Therefore, this article first outlines the trajectory planning algorithm for autonomous vehicles and proposes a new global path planning method. This method combines an improved A * algorithm and a travel time prediction model, taking into account dynamic factors such as traffic congestion and road conditions by predicting the expected time required for crossing the route. The research objective of this article is to verify the effectiveness of the proposed model in accurately planning the trajectory of autonomous vehicles and demonstrate the advantages of bidirectional LSTM networks in predicting road inflow and travel time.

2. Related work

Research In the 1960s, related research on mobile robots was first started, and the first generation of mobile robots was successfully developed. After that, unmanned driving-related technologies have been developed rapidly [8]. In 2016, Waymo began live-testing work on driverless vehicles. The Waymo unmanned vehicle is equipped with a rotary laser rangefinder on the roof. The device can emit 64 laser beams, with a detection range of 200 meters, and a relatively accurate 3D data map can be obtained [9], [10]. The data processing system will fuse the obtained map data with high-precision maps stored internally to calculate multiple data models. The system uses a camera installed on the front windshield for close range detection, which can accurately identify obstacles and pedestrians in the image. And record the environmental information and traffic signs of the road, which can be further integrated and analyzed in the future. Meanwhile, sensors installed on the tires can monitor whether the autonomous vehicle is following a predetermined trajectory. In addition, the system can also achieve safe parking function and quickly calculate the distance to obstacles behind it during reversing [11].

Swarm intelligence algorithms are inspired by the social behavior of natural biological populations and aim to optimize algorithm performance. In this algorithm, individual members learn from each other, share information, and conduct search activities in parallel. Due to the inherent uncertainty of individual and group behavior, the search space exhibits randomness, making it impossible to guarantee the discovery of all efficient itemsets [12]. However, each individual can guide the search direction based on their own fitness value, and they can directly or indirectly interact with other individuals or environments, continuously learn, and iteratively update themselves. During this process, individuals tend to explore in a positive direction, focusing on searching smaller subspaces in order to obtain as much useful information as possible and discover efficient itemsets [13].According to the scope of action, the path planning algorithm is generally divided into local and global planning. Global path planning has a wide range of maps and is generally planned in a static environment [14, 15]. Local path planning is mainly path planning in a dynamic environment, which plays a role in avoiding obstacles. When the vehicle cannot travel according to the global planned path, the local path planning needs to quickly plan a feasible and safe path according to the current environmental information to ensure that it can avoid obstacles after avoiding obstacles [16]. In the case of the path planning algorithm, when the starting and ending positions are known, global path planning can play the role of navigation and constraints for the unmanned vehicle.

Compared to global path planning, local path planning is based on it and aims to generate collision free driving paths in real-time in dynamic driving environments [17-19]. When facing partially or completely unknown local road conditions, the system needs to rely on the perception layer to capture road condition information and surrounding environmental data, and update and correct them in a timely manner according to changes in road conditions. This requires the entire system to have excellent data processing and analysis capabilities, and to be able to provide feedback and adjust path planning results based on environmental information. Through the synergistic effect of global and local factors, autonomous vehicles can find the most suitable driving path [20]. In this process, the A* algorithm is used to calculate the shortest path, while intelligent biomimetic algorithms and sampling algorithms play an important role [21].

Although significant progress has been made in the field of autonomous vehicle path planning, there are still some research gaps. For example, existing methods often have high sensitivity to environmental factors and face challenges in complex road environments. In addition, how to strike a balance between real-time performance and accuracy, as well as how to effectively integrate multiple sensor data to improve the robustness of path planning, are urgent issues that need to be addressed. In response to these research gaps, this paper proposes a new global path planning method that combines an improved A * algorithm and a travel time prediction model. By predicting the expected time required to cross the path, this method takes into account dynamic factors such as traffic congestion and road conditions, adding an layer of adaptability to the path planning process. The proposed method aims to improve the accuracy of path planning, enabling intelligent vehicles to make informed decisions in real-time in complex road environments. Through simulation experiments, the method proposed in this paper has demonstrated significant advantages in accurately planning the trajectory of autonomous vehicles.

3. Research on Global Path Planning Based on Improved A*

3.1. A* algorithm

Current work often focuses on path planning in static environments or only focuses on path planning at a certain level (such as global or local). This study emphasizes the importance of real-time performance and adaptability in dynamic driving environments, especially in local path planning. Real time road condition information and surrounding environment data are obtained through the perception layer, and the path planning results are updated and corrected in a timely manner according to changes in road conditions, ensuring that autonomous vehicles can drive safely and efficiently. The traditional A* algorithm mainly focuses on finding the shortest path, while the method proposed in this paper achieves dynamic adjustment of the path planning process by introducing a travel time prediction model. This combination not only considers the length of the path, but also takes into account dynamic factors such as traffic congestion and road construction that may be encountered during actual driving, thereby improving the accuracy and practicality of path planning. To obtain a more practical algorithm, the grid map of the uniform space decomposition method is used to model the global map information, and then the traditional A* algorithm is improved in efficiency and feasibility of generating a global path.

3.1.1 Establishment of an environmental model

An environment model suitable for the operation of unmanned vehicles is established to facilitate the application of the A* algorithm in path planning. The main principle is to facilitate the storage, processing, use and updating of the driverless car microprocessor. In the environment model, the environment map is evenly divided into several equal parts and filled. Each square cut out uniformly is defined as an obstacle grid or a passable grid. Inflation processing is to inflate the obstacles in the environment map, and the effect is shown in Figure 1.

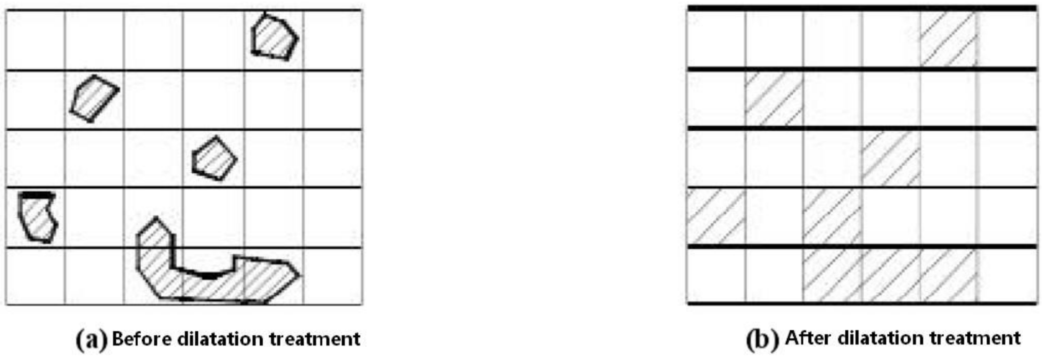
(a) Before dilatation treatment
(b) After dilatation treatment

Figure 1. Environment model building

3.1.2. Path planning process

In the traditional A* algorithm, the heuristic function K(n) is generally defined using the Euclinde-distance. Then the expression of the heuristic function is as follows:

$$K(n)=\sqrt{(x_t-x_n)^2+(y_t-y_n)^2} \quad (1)$$

Then the cost function, when the driverless car travels to n nodes, is

$$p(n)=g(n)+\sqrt{(x_t-x_n)^2+(y_t-y_n)^2} \quad (1.1)$$

Figure 2 shows a uniform grid map of the driving environment of a driverless car, with green, red, blue, and black representing start, endpoints, obstacles, and free-travel space, respectively.

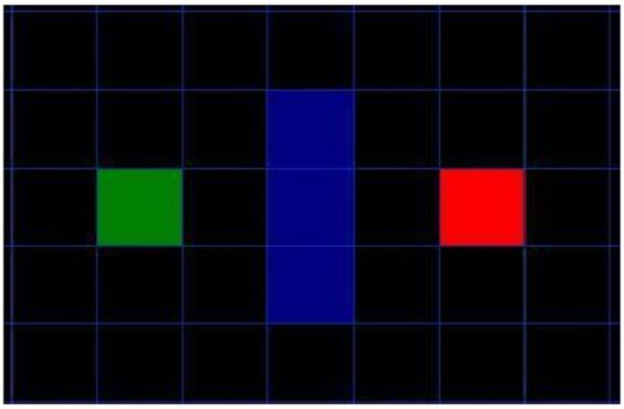

Figure 2. Environment model building

Through the above necessary elements, the shortest path from the starting point to the destination point is solved in these grids. The traditional A* algorithm path planning program flow is shown in Figure 3.

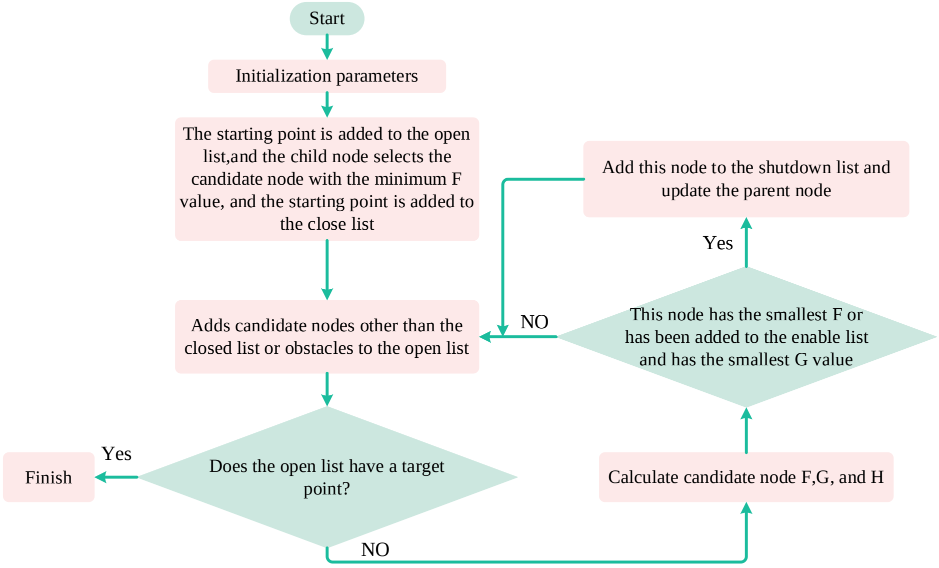
Start
Initialization parameters
The starting point is added to the open list,and the child node selects the candidate node with the minimum F value, and the starting point is added to the close list
Adds candidate nodes other than the closed list or obstacles to the open list
Does the open list have a target point?
Yes
Finish
NO
Calculate candidate node F,G, and H
This node has the smallest F or has been added to the enable list and has the smallest G value
Yes
Add this node to the shutdown list and update the parent node
NO

Figure 3. Traditional A* algorithm path planning

3.2. Improved A* algorithm

3.2.1. Optimizing the heuristic function

When using A* to find the most suitable path, the heuristic function is usually defined by geometric distance, as shown in Formula (1 to 3). From this, it can be known that the planning accuracy and speed of the traditional A* algorithm are static and unchanged during the whole process of path planning. However, the practicality of the heuristic function for geometric distance design is not high. Design of this section

A heuristic function closer to the actual cost value $H(n)$ is obtained, namely:

$$H(n) = \begin{cases} \sqrt{2}d_x(n) + d_y(n) - d_x(n), d_y(n) > d_x(n) \\ \sqrt{2}d_y(n) + d_x(n) - d_y(n), d_y(n) < d_x(n) \end{cases} \tag{2}$$

Although the heuristic function of the traditional A* algorithm has been redesigned above, the speed of path planning has not been changed. Therefore, a controllable factor needs to be added as follows:

$$\mathrm{p(n)=g(n)+(2 - g(n)/}R\mathrm{)k(n)} \tag{2.1}$$

Among them, R is the distance from the starting point to the target point. The accuracy and speed of the improved A* algorithm have been improved.

3.2.2. Sub-node expansion optimization design:

The most primitive A * algorithm is the same when generating its child nodes. Therefore, the characteristics of its child nodes are the same, and the determination of its child nodes and parent nodes ultimately depends on the size of the f value. Therefore, the resulting planned path may pose a risk of friction between autonomous vehicles and obstacle vertices. However, due to the presence of obstacles, their attributes cannot be the same, so we should assign them equal identities to effectively avoid and reduce the occurrence of such situations. As shown in Figure 4, it can be seen that there are eight adjacent nodes (M, N, B, C, Z, Y, E, X) around node Q. Now we will treat them differently and divide (M, N, B, C) into a group called I, which has the highest level; The remaining nodes (Z, Y, E, X) are divided into another group called II, with the lowest level. Because I have the highest level, it is the primary level when generating the current node in a child node. The specific principles are shown in Figure 4:

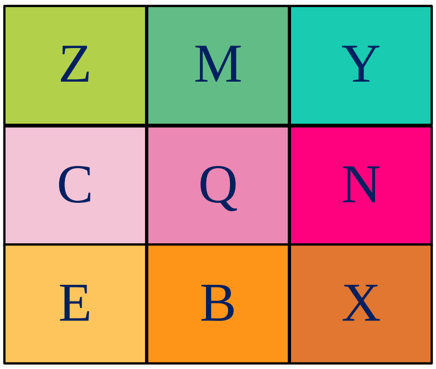

Z	M	Y
C	Q	N
E	B	X

Figure 4. The child node generation strategy of node Q

3.2.3. Floyd algorithm optimization path

The principle of Floyd's algorithm can be represented by a simple mathematical model shown in Figure 5:

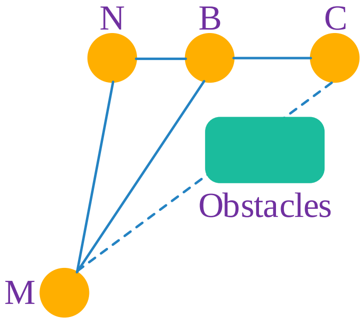

Figure 5. Floyd algorithm principle

L(A,D) is the distance between points M and C. As shown in Figure 5, if there are obstacles in M and C, then you can set L(M,C)=+∞, R(M,C)=M ->C. It can be seen from Figure 5 that point N is the planned node between points M and C like:

$$(M,N)+L(N,C)<L(M.C) \tag{3}$$

But

$$L(M.C)=L(M,N)+L(N,C) \tag{3.1}$$

$$R(M,C)=M\text{-}>N\text{-}>C \tag{3.2}$$

Insert point B between N and C line segments if:

$$L(M,B)+L(B,C)<L(M,N)+L(N,C) \tag{3.3}$$

But

$$L(M.C)=L(M,B)+L(B,C) \tag{3.4}$$

$$R(M,C)=M\text{-}>B\text{-}>C \tag{3.5}$$

Remove point B, then replace the planned path from point M to point C with an optimized arc-shaped path R(M, C) - the path the car travels on.

4. Prediction model of travel time of road segment

4.1. Road segment travel time estimation model construction

Through the relationship between the numerical value and the travel time, a quantitative travel time estimation model is constructed to indirectly obtain the time it takes to pass a road segment with known traffic and known road conditions. The travel time of the road segment is expressed by the travel time of the non-congested road segment and the queuing delay time at the intersection. It is defined as follows:

$$Ca(t)\text{=}Cf(t)\text{+}Cd(t) \tag{4}$$

Among them, $C_a(t)$ represents the travel time (s) of the vehicle entering the road segment a at time t, $C_f(t)$Indicates the travel time (s) of the vehicle in the non-congested part of the road section, $C_d(t)$ Indicates the vehicle's queue delay time (s) at the intersection downstream of road segment a.

According to the relevant theories of traffic engineering, $C_f(t)$ and $C_d(t)$ can be expressed as the incoming flow on road segment a $X_a(t)$ (veh)、outflow $y_a(t)$（veh）、traffic flow $q_a(t)$（veh）, that is, formula (4.1) can be expressed as:

$$Ca(t)\text{=}Ca(xa(t),(ya(t),(qa(t)) \tag{4.1}$$

The incoming flow, outgoing flow and traffic flow of a road segment can be replaced with each other so that it can be further expressed as a function only related to the incoming flow, namely:

$$Ca(t)\text{=}Ca(xa(1),(xa(2),...,(xa(t)) \tag{4.2}$$

Suppose the length of vehicles travelling on a non-congested road section is $L_a^f(t)$, and the length of vehicles queuing at the intersection is $L_a^d(t)$(km), so the length of road section a is

$$La(t)\text{=}Laf(t)\text{+}Lad(t) \tag{4.3}$$

Assume that the vehicle's driving speed is $v_a(t)$(km/h), and according to the relationship between distance, speed and time, it can be known that the vehicle's driving time in a non-congested road section is

$$c_a(t)=\frac{L_a-L_a^d(t)}{v_a(t)} \tag{4.4}$$

Therefore, in order to obtain the time $c_f(t)$ when the vehicle travels on a non-congested road section, it is necessary first to obtain $L_a^d(t)$ the length of the vehicle queuing at the intersection.According to the traffic fluctuation theory, the wave speed of the stop wave before the intersection $\omega_s(t)$(km/h) and the traffic density upstream of the intersection k_a (veh/km/lane)、the blocking density before the intersection k_a^j(veh/km/lane) is related to the free-flow velocity v_a^f(km/h) of the road section as follows:

$$\omega_s(t)\text{=-}v_a^f\cdot\frac{k_a}{k_a^j} \tag{4.5}$$

Suppose the length of the red light at the intersection is r(s), then the distance:

$$|\omega_s(t)|\cdot r \tag{4.6}$$

t that the parking wave moves upstream is:

$$N_a^d(t)=|\omega_s(t)|\cdot r\cdot k_a^j=v_a^f\cdot k_a\cdot r \tag{4.7}$$

The Greenshield speed-density model is shown in Equation (4.8), and the relationship between traffic flow, density and speed is shown in Equation (4.9). According to Equation (4.8) to Equation (4.10), Equation (4.11) is obtained:

$$v_a(t)=v_a^f(1-\frac{k_a}{k_a^j}) \tag{4.8}$$

$$x_a(t)=v_a(t).k_a \tag{4.9}$$

$$\frac{k_a^2}{k_a^j}-k_a+\frac{x_a(t)}{v_a^f}=0 \tag{4.10}$$

$$k_a=\frac{1}{2}k_a^j(1\pm\sqrt{1-4\frac{x_a(t)}{k_a^j.v_a^f}}) \tag{4.11}$$

Among them, it is required $x_a(t)\le\frac{1}{4}k_a^j v_a^f$ that $x_a(t)$ when the value is larger, take the positive sign; when the $x_a(t)$value is smaller, take the negative sign. Therefore, the number of queued vehicles $N_a^d(t)$(veh) at the intersection downstream of the road segment at the moment is

$$N_a^d(t)=\frac{1}{2}k_a^j v_a^f r(1\pm\sqrt{1-4\frac{x_a(t)}{k_a^j.v_a^f}}) \tag{4.12}$$

If the time is discretized, $N_a^d(t)$ and $N_a^d(t+1)$ represent the number of queued vehicles at the intersection downstream$a$ of the road segment at the start timeΔt and end$t$, t+Δt of the time interval, respectively. That is, $N_a^d(t)$ and $N_a^d(t+1)$ are the number of vehicles queuing in continuous time, $N_a^d(t)$represents the number of queued vehicles in discrete time sense, then take the average of the number of queued vehicles in the timeΔt interval, namely

$$N_a^d(t)=\tfrac{1}{2}(N_a^d(t)+N_a^d(t+1))= \\ \frac{1}{4}k_a^j v_a^f r\left\{(1\pm\sqrt{1-4\frac{x_a(t)}{k_a^j.v_a^f}})+(1\pm\sqrt{1-4\frac{x_a(t+1)}{k_a^j.v_a^f}})\right\} \tag{4.13}$$

Since the time interval is too small, $\mathrm{x_a(t)}$ the incoming flow of road segments in adjacent periods and upstream traffic density k_a approximately equal, so

$$N_a^d(t)=\frac{1}{2}k_a^j v_a^f r(1\pm\sqrt{1-4\frac{x_a(t)}{k_a^j.v_a^f}}) \tag{4.14}$$

Let the average vehicle length of vehicles be l_c(km), then the $L_a^d(t)$ length of vehicles queuing at the intersection is

$$L_a^d(t)=N_a^d(t)l_c=\frac{1}{2}v_a^f.r.l_c.k_a^j(1\pm\sqrt{1-4\frac{x_a(t)}{k_a^j.v_a^f}}) \tag{4.15}$$

Known, $N_a^j=\frac{1000_n}{Hd}$, Hd is the average head-to-head distance (km), equal to the sum of the average blocking clearance and the average body length, n is the number of one-way motor vehicle lanes, so the driving time of vehicles in the non-congested road section is

$$c_f(t)=\frac{L_a}{v_a(t)}-500\frac{v_a^f.r.l_c.n\left(1\pm\sqrt{1-\frac{x_a(t)Hd}{250n.v_a^f}}\right)}{v_a(t)Hd} \tag{4.16}$$

The queuing delay time of vehicles at the intersection downstream of the a road section is determined by the number of queuing vehicles and the traffic capacity Q_a(veh) of the intersection.

$$c_d(t) = \frac{N_a^d(t)}{Q_a} = 500\frac{v_a^f.r.n(1 \pm \sqrt{1-\frac{x_a(t)Hd}{250n.v_a^f}})}{Q_aHd} \tag{4.17}$$

Substituting formula (4.16) and formula (4.17) into formula (4.1), the travel time of the vehicle on the entire road a section can be obtained,

$$c_d(t) = \frac{L_a}{v_a(t)} - 500\frac{v_a^f.r.l_c.n\left(1\pm\sqrt{1-\frac{x_a(t)Hd}{250n.v_a^f}}\right)}{v_a(t)Hd} + 500\frac{v_a^f.r.n(1 \pm \sqrt{1-\frac{x_a(t)Hd}{250n.v_a^f}})}{Q_aHd} \tag{4.18}$$

When a vehicle is driving on a non-congested road, it can be considered that the vehicle is almost in a free-flow state, and the driving speed is high $\mathrm{v_a(t)} \approx \mathrm{v_a^f}$. Therefore, in formula (4.18), only the inbound flow $\mathrm{x_a(t)}$ is unknown, and the inbound flow difference between road segments is large, and $\mathrm{x_a(t)}$ needs to be predicted when studying the travel time of road segments in future periods; other parameters can be obtained in advance, or the average value can be used instead. To sum up, we will continue to build a road segment travel time prediction model in the future period and use it to predict the inflow of the road segment in the future period.

4.2. Prediction model for travel time of road segments in the future

The prediction result of travel time is used as the basis for calculating the right of way for route planning, so the accuracy of travel time prediction is closely related to the decision of route planning. LSTM neural network is an algorithm that is widely used in the field of sequence prediction. It can store important past information in the prediction process and ignore unimportant information.

（1）LSTM Neural Network Theoretical Analysis:

LSTM replaces the hidden layer node of the RNN neural network with a memory unit. The structure of the LSTM memory unit module is shown in Figure 6, and the calculation formula (4.19-4.23).

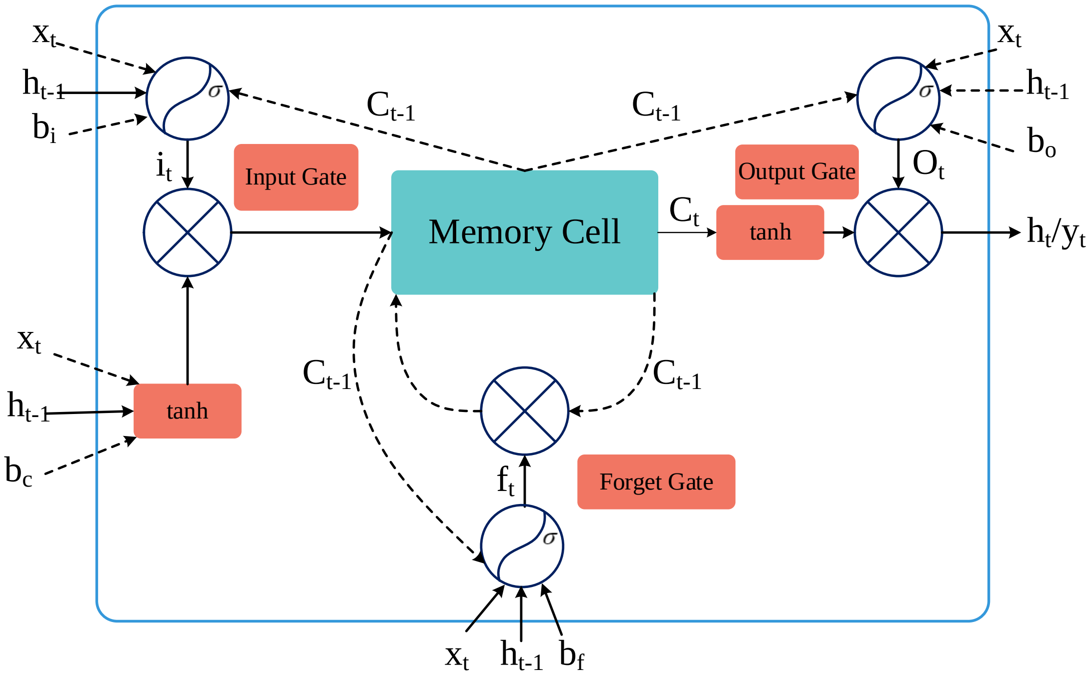

Figure 6. Basic architecture of LSTM memory unit

$$i_t = \sigma(\omega_{xi}x_t + \omega_{hi}h_{t-1} + \omega_{ci}c_{t-1} + b_i) \quad (4.19)$$

$$o_t = \sigma(\omega_{xo}x_t + \omega_{ho}h_{t-1} + \omega_{co}c_{t-1} + o) \quad (4.20)$$

$$f_t = \sigma(\omega_{xf}x_t + \omega_{hf}h_{t-1} + \omega_{cf}c_{t-1} + b_f) \quad (4.21)$$

$$c_t = f_t \odot c_{t-1} + i_t \odot \tan h\,(\omega_{xc}x_t + \omega_{kc}h_{t-1} + b_c) \quad (4.22)$$

$$h_t = o_t \odot \tan h(c_t) \quad (4.23)$$

Among them, x_t and y_t represent the input sequence and output sequence, respectively;i_t、o_t、f_t、c_t and h_t represent the output of the input gate, output gate, forget gate, memory cell and hidden layer at the t moment;ω and b2 represent the weight coefficient matrix and the bias term, respectively; σ(·) and tanh(·) represent the Sigmoid function and the hyperbolic tangent function respectively, which belong to the activation function.

Although LSTM is an improvement over RNN, the memory and learning ability of LSTM is limited, and LSTM cannot encode information from back to front. The traffic volume predicted in this paper has a certain periodicity and regularity. Combining the forward and backward dependencies can extract more traffic volume change characteristics and improve prediction accuracy. Therefore, this time, the bidirectional LSTM neural network is selected for prediction, which is an extension of the traditional LSTM, and the forward and backward time series are trained at the same time to provide the network with contextual information so that the network can learn faster and more fully. The structure is shown in Figure 7.

Among them, $x_t$and$y_t$represent the input sequence and output sequence, respectively, and $\underset{h_t}{\rightarrow}$ and $\underset{h_t}{\leftarrow}$ represent the hidden layer output in forward calculation and backward calculation, respectively. It is concluded that the two hidden layers of the model are independent and non-interfering with each other. The state $\underset{h_t}{\rightarrow}$ and t-1 in the forward hidden layer is related to the state at time -1, and the state at time t+1 in the backward hidden layer is related to the state at time t+1. Status related. The final hidden layer output of the model is formed by linear fusion of the forward hidden layer output sequence and the backward hidden layer output sequence. The calculation formula is shown in formula (4.24).

Among them, $\underset{h_t}{\leftrightarrow}$ represents the final output of the hidden layer, $\underset{\omega_t}{\rightarrow}$ and $\underset{\omega_t}{\leftarrow}$ represents the weight coefficient matrix of forward and backward calculations, respectively, representing the bias term.

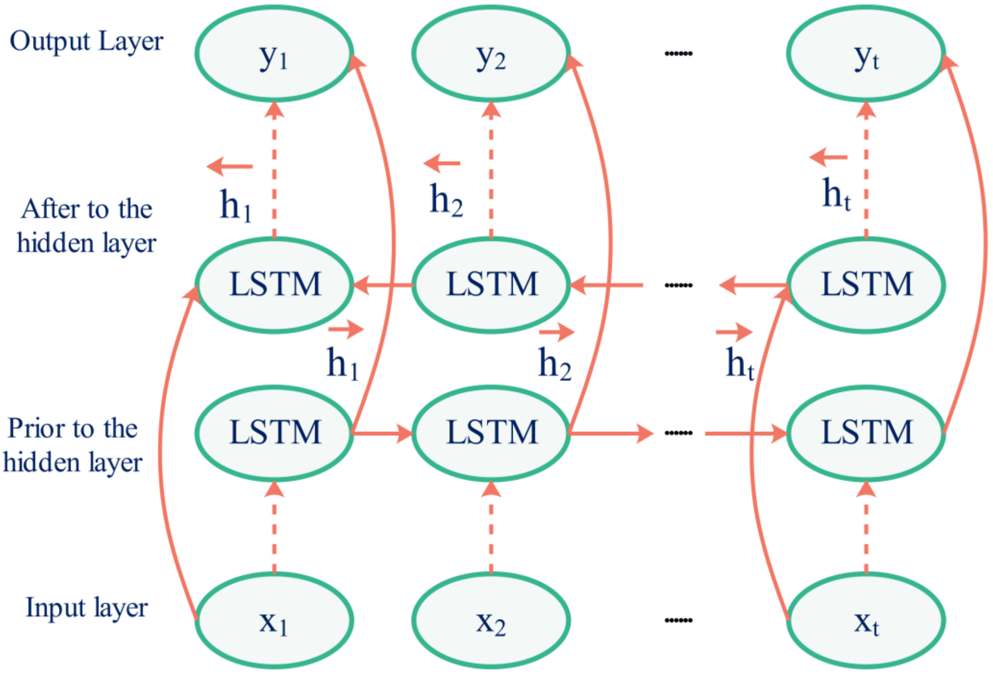

Figure 7. Structure of bidirectional LSTM neural network model

$$\overleftrightarrow{h_t} = \overrightarrow{\omega_t}\overrightarrow{h_t} + \overleftarrow{\omega_t}\overleftarrow{h_t} + \overleftrightarrow{b_t} \quad (4.24)$$

(2) A Road Segment Travel Time Prediction Model with Bidirectional LSTM Neural Networks

For a certain road section of the urban road network, the inflow at the current moment is related to the traffic data, such as the inflow $x_i(i<t)$, speed $v_i(i<t)$ and occupancy $\theta_i(i<t)$ of the road section at the previous moment, so inputting the historical traffic data X can predict the road section at the next moment into the flow. Therefore, inputting the historical traffic data X can predict the inflow of the road segment at the next moment. Considering the impact of the incoming flow, speed and occupancy rate at the previous moment on the incoming flow x_{n+1} therefore, X is an N×3 matrix in the future and the above prediction problem can be simplified as the formula.

$$X=\begin{bmatrix} x_1 & v_1 & \theta_1 \\ x_2 & v_2 & \theta_2 \\ \vdots & \vdots & \vdots \\ x_N & v_N & \theta_N \end{bmatrix} \tag{4.25}$$

$$x_{N+1} = predictor(X) \tag{4.26}$$

The LSTM model mainly has parameters such as weight coefficient and bias. The setting can be obtained by training the input data; other parameters must be set manually. The traffic data at intervals of 5 minutes is used for prediction, the input time series step timesteps are set to 12, and the forecast time series step size is set to 1. That is, the data of 60 minutes is used to predict the data of 5 minutes in the future. The input matrix dimension is 12x3, and the output layer dimension is set to 1. Studies have shown that the neural network's learning ability with more hidden layers is stronger, the neural network is more prone to overfitting, and the training time will be greatly increased. This paper adopts a four-layer network design, including an input layer, a bidirectional LSTM layer, a fully connected layer (Dense layer) and an output layer.

The forward LSTM layer contains 64 hidden units, the backward LSTM layer contains 64 hidden units, and the Dense layer contains 1 neuron. The Dropout method can randomly deactivate some neurons in the hidden layer during the training process, reduce the complex dependencies between neurons, improve the model's generalization ability, and avoid overfitting the model during the training process. The dropout rate is set to 0.2. The structure of the prediction model constructed in this paper is shown in Figure 8.

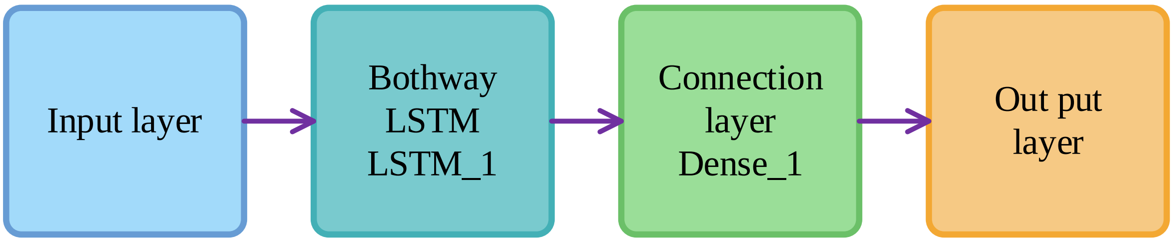

Figure 8. Structure diagram of two-way LSTM prediction model

The algorithm steps for predicting future incoming flows with a bidirectional LSTM neural network are as follows:

Step 1: Data preprocessing. Process outliers and missing values in the data, post-normalize the data and divide the training and test sets.

Step 2: Build a road segment travel time prediction model in the future period, and initialize the model parameters. Set the number of hidden layers, the number of fully connected layers, the number of neurons in each layer, the learning step size, the number of iterations, the dropout loss value, the optimization function and other parameter values of the bidirectional LSTM model, and randomly set the weight coefficient matrix and bias item.

Step 3: Model training and testing. Input the training data set, train the model, train and iterate repeatedly until the model's prediction accuracy reaches the preset accuracy, and then denormalize the data output by the model.

Step 4: Input the historical traffic data of the road network to obtain the dynamic road resistance function. The process is shown in Figure 9.

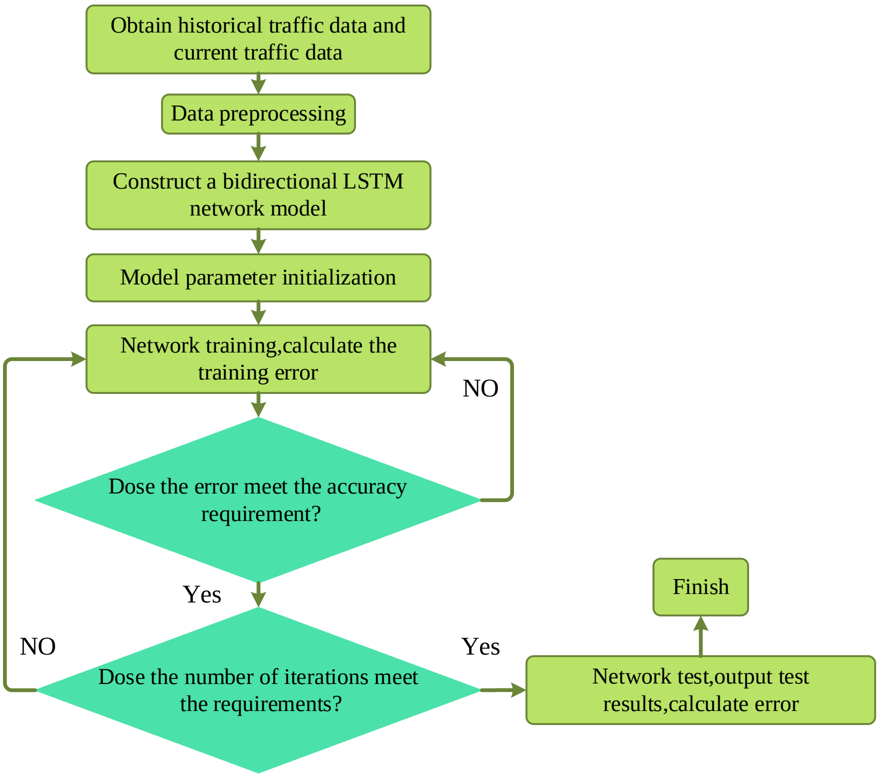
Obtain historical traffic data and current traffic data
Data preprocessing
Construct a bidirectional LSTM network model
Model parameter initialization
Network training,calculate the training error
NO
Dose the error meet the accuracy requirement?
Yes
Finish
NO
Yes
Dose the number of iterations meet the requirements?
Network test,output test results,calculate error

Figure 9. Flow chart of bidirectional LSTM network algorithm

4.3. Empirical Analysis of Travel Time Prediction of Road Sections in Future Periods

In order to evaluate the validity and practicality of the model, the traffic data of the road network is collected for algorithm testing. The data was collected in a cycle of 30s, from March 1st to April 28th, 2020, for a total of 59 days. According to previous studies, traffic flow data with an interval of 5 minutes is more suitable for short-term traffic flow prediction because the proportion of missing data is small. Therefore, the data is aggregated at 5min intervals. The first 70% of the data is used as the training set, and the last 30% of the data is used as the test set.

(1) Evaluation indicators

The mean absolute error MAE, the mean absolute percentage error MAPE and the root mean square error RMSE were selected as evaluation indicators. MAE can well reflect the actual situation of the predicted value error, MAPE can reflect the model's overall accuracy, and RMSE can evaluate the adaptability of the data and prediction model. value; $\mathrm{x_k}$ is the actual value; x'_k is the predicted value.

$$MAE = \frac{1}{n}\sum_{k=1}^{n}|x_k - x'_k| \tag{4.27}$$

$$MAPE = \frac{1}{n}\sum_{k=1}^{n}\left|\frac{x_k - x'_k}{x_k}\right| \tag{4.28}$$

$$RMSE = \sqrt{\frac{1}{n}\sum_{k=1}^{n}(x_k - x'_k)^2} \tag{4.29}$$

(2) Analysis of results

The traditional BP neural network (referred to as "BPNN"), the BP neural network optimized by genetic algorithm (referred to as "GABPNN") and the traditional LSTM neural network are selected for comparative experiments. The prediction results of the bidirectional LSTM neural network are shown in Figure 10. The prediction errors of different models are shown in Table 1, and the training time of different models is shown in Table 2.

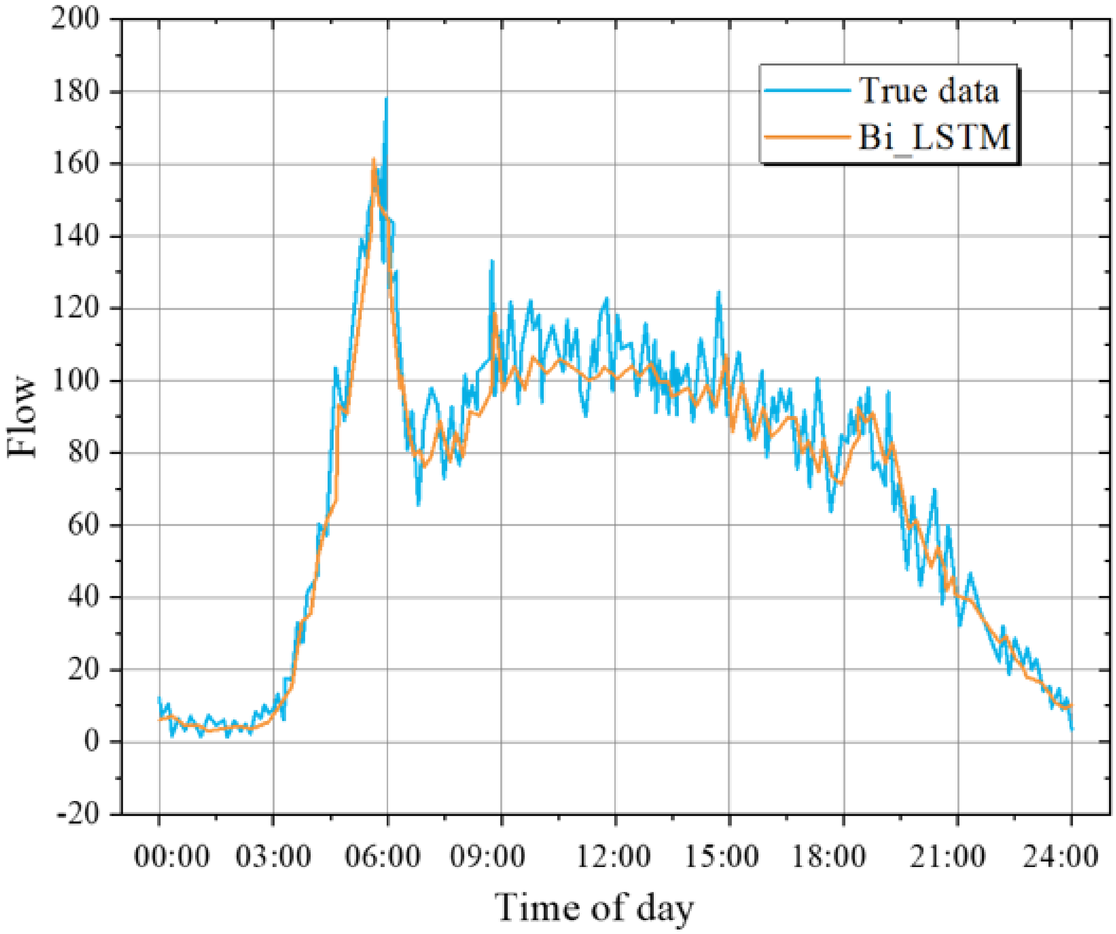

Figure 10. Prediction results of bidirectional LSTM network

Table 1. Prediction errors of different models

Model	MAE	MAPE	RMSE
BNPP	10.7621	0.2644	15.2133
GABPNN	9.4671	0.2561	9.8535
LSTM	7.6692	0.1682	9.9697
two-way LSTM	7.3165	0.1632	9.9162

Table 2. Training time of different models

Model	Training time(s)
BNPP	50
GABPNN	399
LSTM	117
two-way LSTM	181

The results show that, compared with the other three models, the bidirectional LSTM model has better prediction results, the predicted value is closer to the real value, the prediction performance is more stable, and it has higher adaptability to different traffic flow conditions. Based on the prediction model constructed above, the road segment inflow in the future period can be predicted in real time and accurately, and the travel time of the road segment in the future period can be calculated.

Based on the prediction results of the bidirectional LSTM model, autonomous vehicles can accurately predict the inflow of road segments in real time and calculate the travel time of a future road segment accordingly. This real-time prediction capability is crucial for the path planning of autonomous vehicles, as it allows vehicles to dynamically adjust their driving routes based on current and future traffic conditions. This not only improves the efficiency and accuracy of path planning, but also enhances the ability of autonomous vehicles to respond to unexpected situations. In addition, the application of bidirectional LSTM models in predicting road travel time can further promote the development of intelligent transportation systems. By integrating the predicted results into the intelligent transportation system, more accurate traffic flow management and control can be achieved. For example, adjusting signal timing and optimizing traffic diversion plans based on prediction results can effectively alleviate traffic congestion and improve road capacity. This application not only improves the overall efficiency of urban transportation, but also provides a more complete transportation environment for the widespread application of autonomous vehicles.

5. Conclusion

The improved path planning algorithm proposed in this study significantly overcomes the two main shortcomings of the original algorithm, achieving a dual improvement in accuracy and speed. By optimizing the turning strategy, we have verified the effectiveness and rationality of the Floyd algorithm in reducing turning angles and the number of nodes, and stabilizing the planned path, thereby significantly shortening the length of the planned path and reducing planning time. In addition, the heuristic function we designed not only improves the accuracy of path search, but also accelerates the search speed, significantly reducing the number of nodes traversed, among which the design of sub node expansion strategy plays a crucial role. More importantly, based on improving the accuracy and simplicity of the algorithm, this study constructed a road segment travel time estimation model and a prediction model. Based on these models, we innovatively constructed a segmented dynamic road resistance function that can predict the travel time of vehicles when they reach each road segment in the future. This feature provides real-time data reference for autonomous vehicles, enabling them to dynamically plan the optimal path from their current location to their destination. These improvements not only enhance the performance of path planning algorithms, but also greatly improve their reliability and practicality in practical applications. By comprehensively considering multiple factors such as travel time, turning stability, and path length, this study provides new ideas and methods for intelligent navigation and path planning of autonomous vehicles.

Competing of interests

The authors declare no competing of interests.

Authorship Contribution Statement

Dandan Song: Writing-Original draft preparation, Conceptualization, Supervision, Project administration.

Tao Yang: Methodology, Software, Validation.

References

[1] Tomoyuki Muto, Hiroaki Inui, Hiroki Ninomiya, Masahiko Komai, Yoshiaki Kanatani *et al.*, 'Factors affecting clinical outcomes after massive rotator cuff repair using a data mining technique', *Journal of Shoulder and Elbow Surgery*, Vol. 31, No. 4, p. e210, April 2022, ISSN: 1058-2746, DOI: 10.1016/j.jse.2022.01.107, Available: https://www.jshoulderelbow.org/article/S1058-2746(22)00139-2/abstract.

[2] Massimo Bertozzi, Alberto Broggi, Alessandro Coati and Rean Isabella Fedriga, 'A 13,000 km intercontinental trip with driverless vehicles: The VIAC experiment', *IEEE Intelligent Transportation Systems Magazine*, Vol. 5, No. 1, pp. 28–41, 24 January 2013, Electronic ISSN: 1941-1197, DOI: 10.1109/MITS.2012.2225651, Available: https://ieeexplore.ieee.org/abstract/document/6420052.

[3] Ronald Kline and Trevor Pinch, 'Users as agents of technological change: The social construction of the automobile in the rural United States', *Technology and culture*, Vol. 37, No. 4, pp. 763–795, October 1996, ISSN: 1097-3729, DOI: 10.1353/tech.1996.0006, Available: https://muse.jhu.edu/article/887403.

[4] Mohammed Shafi Kundiladi, Sheik Masthan Shahul Abdul Rahim and Mohammed Shahal Rishad, "Secure Autonomous Vehicle Localization Framework using GMCC and FSCH-KMC under GPS-Denied Locations", *Annals of Emerging Technologies in Computing (AETiC)*, Print ISSN: 2516-0281, Online ISSN: 2516-029X, pp. 64-74, Vol. 8, No. 3, 1st July 2024, Published by International Association for Educators and Researchers (IAER), DOI: 10.33166/AETiC.2024.03.005, Available: http://aetic.theiaer.org/archive/v8/v8n3/p5.html.

[5] Turki Y Abdalla, Ali A Abed and Alaa A Ahmed, 'Mobile robot navigation using PSO-optimized fuzzy artificial potential field with fuzzy control', *Journal of Intelligent & Fuzzy Systems*, Vol. 32, No. 6, pp. 3893–3908, 23rd May 2017, ISSN: 1064-1246, DOI: 10.3233/IFS-162205, Available: https://content.iospress.com/articles/journal-of-intelligent-and-fuzzy-systems/ifs2205.

[6] Thierry Fraichard and Hajime Asama, 'Inevitable collision states—a step towards safer robots?', *Advanced Robotics*, Vol. 18, No. 10, pp. 1001–1024, 2nd April 2004, ISSN: 0169-1864, DOI: 10.1163/1568553042674662, Available: https://www.tandfonline.com/doi/abs/10.1163/1568553042674662.

[7] Andrei Lissovoi and Carsten Witt, 'Runtime analysis of ant colony optimization on dynamic shortest path problems', in *Proceedings of the 15th Annual Conference on Genetic and Evolutionary Computation*, 6-10 July 2013, Amsterdam, The Netherlands, pp. 1605–1612, Publisher: Association for Computing Machinery, ISBN: 9781450319638, DOI: 10.1145/2463372.2463567, Available: https://dl.acm.org/doi/abs/10.1145/2463372.2463567.

[8] Haibin Duan, Pei Li, Yuhui Shi, Xiangyin Zhang and Changhao Sun, 'Interactive learning environment for bio-inspired optimization algorithms for UAV path planning', *IEEE Transactions on Education*, Vol. 58, No. 4, pp. 276–281, 10th March 2015, ISSN: 0018-9359, DOI: 10.1109/TE.2015.2402196, Available: https://ieeexplore.ieee.org/abstract/document/7057693.

[9] Hyejeong Ryu and Younghoon Park, 'Improved informed RRT* using gridmap skeletonization for mobile robot path planning', *International Journal of Precision Engineering and Manufacturing*, Vol. 20, pp. 2033–2039, 11th September 2019, ISSN: 2234-7593, DOI: 10.1007/s12541-019-00224-8, Available: https://link.springer.com/article/10.1007/s12541-019-00224-8.

[10] Chongsheng Zhang, George Almpanidis, Wanwan Wang and Changchang Liu, 'An empirical evaluation of high utility itemset mining algorithms', *Expert Systems with Applications*, Vol. 101, pp. 91–115, 1st July 2018, Online ISSN: 1873-6793, Print ISSN: 0957-4174, DOI: 10.1016/j.eswa.2018.02.008, Available: https://www.sciencedirect.com/science/article/abs/pii/S0957417418300782.

[11] Wei Song, Chunhua Wang and Jinhong Li, 'Binary partition for itemsets expansion in mining high utility itemsets', *Intelligent Data Analysis*, Vol. 20, No. 4, pp. 915–931, 15th June 2016, ISSN: 1088-467X, DOI: 10.3233/IDA-160838, Available: https://content.iospress.com/articles/intelligent-data-analysis/ida838.

[12] Wei Song, Yu Liu and Jinhong Li, 'BAHUI: fast and memory efficient mining of high utility itemsets based on bitmap', *International Journal of Data Warehousing and Mining (IJDWM)*, Vol. 10, No. 1, pp. 1–15, 2014, Publisher: IGI Global, USA, ISSN: 1548-3924, DOI: 10.4018/ijdwm.2014010101, Available: https://www.igi-global.com/article/bahui/106859.

[13] K Indira, S Kanmani, V Ashwini, B Rangalakshmi, P Divya Mary *et al.*, 'Mining association rules using adaptive particle swarm optimization', in *Proceedings of the International Conference on Advanced Computing, Networking, and Informatics*, New Delhi, India, 12th – 14th June 2013, pp. 975–984, ISSN: 8132216644, DOI: 10.1007/978-81-322-1665-0_99, Available: https://link.springer.com/chapter/10.1007/978-81-322-1665-0_99.

[14] Gengxin Sun and Chih-Cheng Chen, 'Influence maximization algorithm based on reverse reachable set', *Math Problems in Engineering*, Vol. 2021, pp. 1–12, 28th July 2021, ISSN: 1563-5147, DOI: 10.1155/2021/5535843, Available: https://onlinelibrary.wiley.com/doi/full/10.1155/2021/5535843.

[15] Jerry Chun-Wei Lin, Lu Yang, Philippe Fournier-Viger, Jimmy Ming-Thai Wu, Tzung-Pei Hong *et al.*, 'Mining high-utility itemsets based on particle swarm optimization', *Engineering Applications of Artificial Intelligence*, Vol. 55, pp. 320–330, October 2016, ISSN: 0952-1976, DOI: 10.1016/j.engappai.2016.07.006, Available: https://www.sciencedirect.com/science/article/abs/pii/S0952197616301312.

[16] Soroor Malekmohamadi Faradonbe and Faramarz Safi-Esfahani, 'A classifier task based on Neural Turing Machine and particle swarm algorithm', *Neurocomputing*, Vol. 396, pp. 133–152, 5th July 2020, Online ISSN: 1872-8286, , Print ISSN: 0925-2312DOI: 10.1016/j.neucom.2018.07.097, Available: https://www.sciencedirect.com/science/article/abs/pii/S0925231219304278.

[17] Hussam N Fakhouri, Amjad Hudaib and Azzam Sleit, 'Multivector particle swarm optimization algorithm', *Soft Computing*, Vol. 24, No. 15, pp. 11695–11713, 23rd December 2019, ISSN: 1432-7643, DOI: 10.1007/s00500-019-04631-x, Available: https://link.springer.com/article/10.1007/s00500-019-04631-x.

[18] Le Sun and Congmou Zhu, 'Impact of Digital Inclusive Finance on Rural High-Quality Development: Evidence from China', *Discrete Dynamics in Nature and Society*, Vol. 2022, No. 1, p. 7939103, 23rd August 2022, ISSN: 1607-887X, DOI: 10.1155/2022/7939103, Available: https://onlinelibrary.wiley.com/doi/full/10.1155/2022/7939103.

[19] Jimmy Ming-Tai Wu, Justin Zhan and Jerry Chun-Wei Lin, 'An ACO-based approach to mine high-utility itemsets', *Knowledge-Based Systems*, Vol. 116, pp. 102–113, 2017, ISSN: 0950-7051, DOI: 10.1016/j.knosys.2016.10.027, Available: https://www.sciencedirect.com/science/article/abs/pii/S0950705116304191.

[20] Mehdi Neshat, Ghodrat Sepidnam, Mehdi Sargolzaei and Adel Najaran Toosi, 'Artificial fish swarm algorithm: a survey of the state-of-the-art, hybridization, combinatorial and indicative applications', *Artificial Intelligence Review*, Vol. 42, No. 4, pp. 965–997, 15th January 2017, ISSN: 0269-2821, DOI: 10.1007/s10462-012-9342-2, Available: https://link.springer.com/article/10.1007/s10462-012-9342-2.

[21] Yi Liu, Xuesong Feng, Lukai Zhang, Weixing Hua and Kemeng Li, 'A pareto artificial fish swarm algorithm for solving a multi-objective electric transit network design problem', *Transportmetrica A: Transport Science*, Vol. 16, No. 3, pp. 1648–1670, 8th November 2019, ISSN: 2324-9935, DOI: 10.1080/23249935.2020.1773574, Available: https://www.tandfonline.com/doi/abs/10.1080/23249935.2020.1773574.